Joint Transmission in Indoor Visible Light Communication Downlink Cellular Networks

Cheng Chen*, Dobroslav Tsonev* and Harald Haas*
*Institute for Digital Communications
The University of Edinburgh EH9 3JL, Edinburgh, UK
{cheng.chen, d.tsonev, h.haas}@ed.ac.uk

***Abstract*—In future visible light communication (VLC) systems, networked multi-cell operation is required to achieve seamless coverage and high data rate in typical indoor environments. We refer to this type of cellular network as optical atto-cell network. In such network, co-channel interference (CCI) between adjacent optical atto-cells limits the performance of the network. In order to maximise system throughput and improve signal quality in the whole coverage area, it is necessary to mitigate CCI. In this paper, the concept of multi-point joint transmission (JT) is adapted to a VLC cellular network. It can generally be described as concurrent data transmission from multiple cooperating base stations (BSs) to a mobile station (MS). In a VLC JT system, strong CCI is avoided by co-ordinated transmission and, in addition, we exploit a particular characteristic of intensity modulation (IM) systems. This is that signals always superimpose constructively which is in stark contrast to radio frequency (RF)-based systems. Therefore, the cell-edge user signal to interference plus noise ratios (SINRs) can be improved. The results show that the JT scheme improves the median SINR by 16.4 dB compared to a full frequency reuse system. Additionally, a JT system exhibits a 67.6% improvement in terms of median system throughput compared to a static resource partitioning system with a reuse factor of 3.**

***Index Terms*—visible light communications, joint transmission, co-channel interference and orthogonal frequency division multiple access.**

I. Introduction

Recent work has shown that optical wireless (OW) technology has significant potential to provide high speed wireless transmission in an indoor environment [1]. In addition, an OW system uses unregulated bandwidth and can be applied where radio frequency (RF) transmission is restricted. Therefore, OW is a suitable candidate for a complementary technology to RF communications. Inexpensive light emitting diodes (LEDs) and photo diodes (PDs) can serve as front-end elements. Visible light communication (VLC) technology has the potential to realise the functions of illumination and data transmission at the same time. This could lead to lower installation costs and improved power efficiency. In order to achieve communication to multiple roaming mobile stations (MSs) in an office or home indoor environment, a cellular network composed of small optical atto-cells is proposed. The goal is to achieve seamless coverage and high spectral efficiency. An optical atto-cell network can be realised by installing multiple LED access points (APs) in the ceiling of a room with careful alignment. Each AP acts as a base station (BS) and covers the users within its illumination region. If a MS moves out of the coverage region of an AP, handover techniques will guarantee seamless wireless service provision by ensuring that the MS is always served by the most suitable AP.

In an optical atto-cell network, using the same frequency resources in adjacent cells causes co-channel interference (CCI). This significantly degrades the signal to interference plus noise ratio (SINR) available to a cell-edge user, thereby resulting in high outage probability and low data rate. Therefore, interference coordination techniques are required to mitigate CCI. Several approaches are considered in the literature. The simplest approach is applying traditional static resource partitioning [2] by splitting cells into clusters. Within a cluster, frequency resources are allocated in an orthogonal fashion. In this manner, interfering users are separated in space to mitigate CCI. Decreased available bandwidth in each cell is the main drawback of this approach, which significantly limits the user data rate. A busy-burst-based self-organised interference coordination technique is proposed in [3]. It uses the uplink signal to acquire channel information and applies a dynamic interference-aware resource allocation scheme. The busy-burst signalling approach shows significant improvements in terms of fairness and spectral efficiency relative to the static resource partitioning approach. Another technique to mitigate CCI is to adapt the concept of joint transmission (JT) [4] to optical atto-cell networks. In a JT system, a MS can be served by multiple nearby BSs, thereby improving the acquired signal quality. Since this approach substitutes interference signals with desired signals, the received SINR can be significantly improved, especially for the cell-edge MSs. However, many challenges such as backhaul constraints, accurate

978-1-4799-2851-4/13/$31.00 ©2013IEEE

synchronisation and multi-path fading effects limit the performance of JT systems. In a VLC system, due to the special features of intensity modulation and direct detection (IM/DD) [5], it is possible to overcome these difficulties in an optical atto-cell network. The authors in [6] demonstrate that it is possible to achieve a multi-point cooperative transmission scheme in a single user VLC system in a small indoor environment with improved optical power gain and reduced bit error rate (BER). The contribution of this work is to adapt JT to the downlink transmission in an optical atto-cell network in order to mitigate CCI and improve the cell-edge user performance in terms of received SINR and system throughput.

The remainder of the paper is organised as follows. Section II describes the system models. Section III describes the proposed JT scheme. This includes the system characteristics, JT framework and frequency resource planning. Section IV presents the simulation results and discussions. Finally, we conclude the paper in section V.

II. System Model

The system of interest is deployed in a large indoor environment. The entire coverage area is divided into N_{ap} cells with hexagonal shape. N_{ap} BSs each equipped with an LED array are located at the centres of their corresponding cells providing two-way communication to MSs. Each LED array is composed of 7 LED clusters. Since a single LED cannot provide sufficient optical power for communication or illumination, multiple low power LEDs with the same beam direction form a high power LED cluster, which works as a large LED to reach the required power level. Despite the small half-power semiangle of a single LED (20° LED semiangle at half power), each cluster has a slightly different beam direction to cover a different small region of the total coverage area. Each LED cluster is denoted by a tuple $v = (i, n)$ showing that it is the i_{th} LED cluster within the n_{th} LED array, where $i \in [1, 2, \cdots, 7]$ and $n \in [1, 2, \cdots, N_{\mathrm{ap}}]$. Direct-current-biased optical orthogonal frequency division multiplexing (DCO-OFDM) [7] is used in order to realise orthogonal frequency division multiple access (OFDMA) which provides the means to achieve multiple access and combat inter-symbol interference (ISI).

A. Channel

Due to the employment of highly directional LEDs, the signal power from reflected paths is low. Besides, a cyclic prefix is considered in the OFDM frame which mitigates the impact of inter-symbol interference (ISI) and a single tap equaliser can be used. Therefore, the optical channel can be accurately approximated by the line-of-sight (LOS) path. It is valid to consider the channel DC gain only. The channel DC gain G from an LED to a PD detector is given by [5],

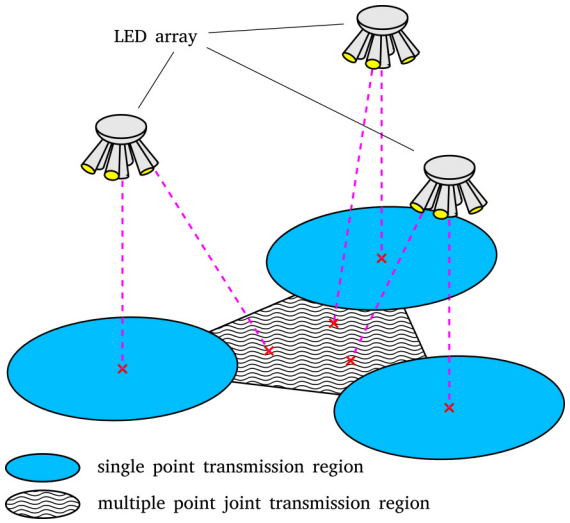

Fig. 1. Multi-point joint transmission.

$$G = \frac{(m+1)A}{2\pi d^2} \cos^m(\phi) T_{\mathrm{s}}(\psi) g_{\mathrm{c}}(\psi) \cos(\psi), \quad (1)$$

where A denotes the physical area of the PD detector; d is the distance between the LED and the PD detector; ϕ represents the radiation angle at the transmitter side; ψ represents the incidence angle at the receiver side; $T_{\mathrm{s}}(\psi)$ models the optical filter gain which is assumed to be 1 in this work; $g_{\mathrm{c}}(\psi)$ denotes the concentrator gain and m is the Lambertian emission order. The ideal concentrator has a gain of:

$$g_{\mathrm{c}}(\psi) = \begin{cases} \frac{n^2}{\sin^2 \Psi_{\mathrm{c}}} & 0 \le \psi \le \Psi_{\mathrm{c}}, \\ 0 & \psi > \Psi_{\mathrm{c}}, \end{cases} \quad (2)$$

where Ψ_{c} models the receiver FOV and n denotes the internal refractive index. The Lambertian emission order is related to the transmitter semiangle at half-power $\Phi_{1/2}$ by $m = -\ln(2)/\ln(\cos(\Phi_{1/2}))$.

B. OFDMA

In an OFDM system, the modulation symbols are converted to OFDM symbols by using the inverse discrete Fourier transform (IDFT) of size K as follows:

$$x_t = \frac{1}{\sqrt{K}} \sum_{k=0}^{K-1} x_k \exp\left(j \frac{2\pi}{K} tk\right), \quad (3)$$

where x_k denotes each of the K data symbols that are used to compose the OFDM symbol, x_t. Due to the requirement for real-valued OFDM symbols, a Hermitian symmetry constraint must be imposed in the frequency domain. Therefore, only half of the total subcarriers

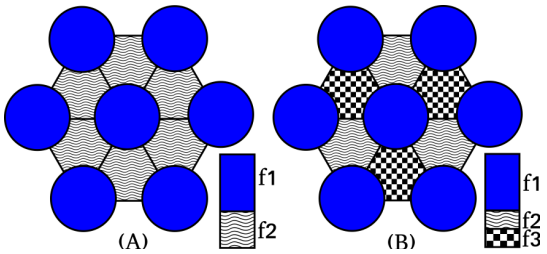

Fig. 2. Plot A and B are the joint transmission frequency plan 1 and 2, respectively.

carry information. Multiple access is realised by allocating different subcarriers to different users. Additionally, a DC-bias and signal clipping are introduced to ensure that the OFDM symbols are positive. The DC-bias and signal clipping are set in a manner that the additional noise is negligible [8]. Although the DC bias carries no information, this portion of power is not wasted since the luminous power must be high enough to meet the illumination requirement. The illuminance should be at least 400 lx for reading purposes [9].

C. SINR

SINR is used as the metric to evaluate the received signal quality at a specified user on each of the allocated subcarriers. The received SINR $\gamma_k(u)$ of MS u on subcarrier k is defined as [10]

$$\gamma_k(u) = \frac{\left(\sum_{v\in V(u)} N_{\mathrm{l}} P_{\mathrm{opt},k} R_{\mathrm{pd}} G_{v,u}\right)^2 F_{\mathrm{OE}}}{\sum_{\hat{u}\neq u}\left(\sum_{\hat{v}\in V(\hat{u})} N_{\mathrm{l}} P_{\mathrm{opt},k} R_{\mathrm{pd}} G_{\hat{v},u}\right)^2 F_{\mathrm{OE}} + \sigma^2}, \tag{4}$$

where N_{l} denotes the number of LEDs per cluster; $P_{\mathrm{opt},k}$ is the optical power of an LED used on subcarrier k; $V(u)$ is the set which contains all the tuples of LED clusters serving user u, and the number of the serving LED clusters for a user varies from 1 to 3; R_{pd} models the PD responsitivity; $G_{v,u}$ is the channel DC gain from LED cluster v to MS u; $\hat{u}$ denotes the users that reuses the same subcarrier k in the system, F_{OE} is the optical to electrical conversion factor and σ^2 represents the electrical additive white Gaussian noise (AWGN) power on each subcarrier. The noise power is dominated by ambient light shot noise and receiver thermal noise. The effects of other noise sources such as clipping noise are omitted since their contribution is negligible. Therefore, the noise power is defined by [3],

$$\sigma^2 = 2qI_{\mathrm{bg}}B_{\mathrm{sc}} + \frac{4K_{\mathrm{b}}TB_{\mathrm{sc}}}{R_{\mathrm{f}}}, \tag{5}$$

where q is the charge of an electron; I_{bg} denotes the current due to background light; B_{sc} denotes the bandwidth of a subcarrier; K_{b} is the Boltzmann constant; T models the absolute temperature and R_{f} is the feedback resistance of the transimpedance amplifier (TIA).

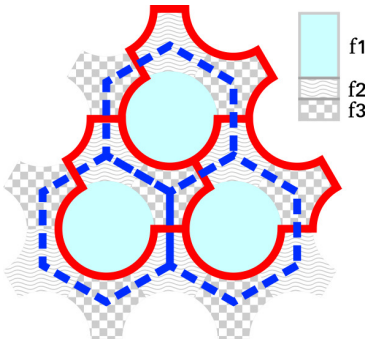

Fig. 3. The area of the region specified by the blue dashed lines (cell coverage area) equals the area of the region specified by the red solid curves. This implies that the JT2 system has the same reuse factor as that of a full frequency reuse system.

In this paper, the downlink user capacity is computed using the Shannon-Hartley theorem:

$$C(u) = \sum_{k\in M(u)} B_{\mathrm{sc}} \log_2(1+\gamma_k(u)), \tag{6}$$

where $M(u)$ represents the set of subcarriers allocated to user u. Lowpass frequency response and non-linear current to optical power transfer function of the LED are not considered here in order to simplify the system model. It is assumed that the detrimental impact of these imperfections are reduced by a proper system design [8].

III. Joint Transmission in VLC

A. Characteristics

In an optical atto-cell network, many system specific properties support the implementation of JT: 1) a very high-speed low-latency connection between BSs is easy to realise due to the short physical distance between BSs; 2) there is no fading effect in IM/DD systems due to constructive combination of intensity modulated signals; Therefore, extra coding and strict synchronisation requirement are unnecessary; 3) since only the LOS path is significant, the time differences between the arrival of signal components from different BSs are small relative to a symbol period; 4) an OFDM-based system has an inherent ability to combat ISI. Applying JT not only improves the communication quality at cell-edges, but also makes the connection more reliable. Since three LOS channels exist simultaneously as a result of the proposed cellular structure, data connection can still be guaranteed for the case that one or two LOS paths are blocked.

B. Framework

Fig. 1 shows the JT system model assumed in this paper. Among the 7 LED clusters in an LED array, the central one works in the single point transmission mode

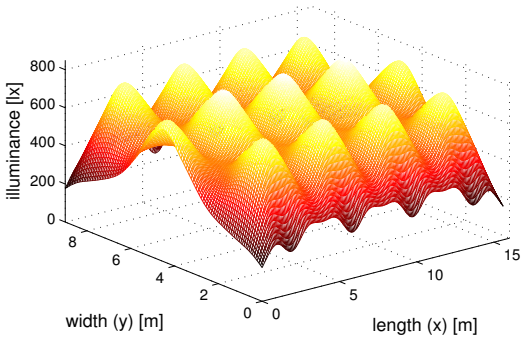

Fig. 4. Illuminance distribution.

TABLE I

Parameters	Symbol	Values
Equivalent LED optical power	P_{opt}	63 [mW]
LED semiangle at half-power	$\Phi_{1/2}$	20°
LED centre luminous intensity	$I(0)$	57.7 [cd]
Number of LEDs per cluster	N_{l}	40
PD responsitivity	R_{pd}	0.28 [A/W]
PD physical area	A	1.5 [cm^2]
Receiver field of view	Ψ_c	70°
LED modulation bandwidth	W	20 [MHz]
JT SINR threshold	γ_{th}	10 dB
Current due to background light	I_{bg}	5100 [μA]
Feedback resistance of TIA	R_{f}	6 [kΩ]
LED cluster beam direction angle	α	38.13°
E/O conversion factor	F_{OE}	1/9

covering the users in the cell-centre. Each of the other 6 exterior LED clusters in an array faces one of the 6 vertices of the hexagonal cell. Since every three adjacent cells have a common vertex, three exterior LED clusters from different adjacent arrays cover a cell corner region. This region is defined as a JT region which is centred at a vertex of a cell. Since there are 6 corners in each cell, there are six JT regions around an LED array. We assume that the system has an uplink system in order to allow MSs to communicate with BSs, and each MS is able to determine the downlink signal strength.

The working mechanisms of the system are described as follows: 1) the central LED cluster of each array transmits a pilot signal to all MSs with a unique sequence to identify the corresponding LED array; 2) each MS selects the BS providing the strongest signal as a primary BS and selects the BSs providing the second and the third strongest signals as the secondary BSs; 3) a MS estimates the received SINR by considering the signal from the primary BS as a desired signal and the other signals as interference; 4) if the SINR is above a predetermined threshold which determines the maximum BER for reliable data transmission, the user replies to the BSs through uplink channel requesting single point transmission from the primary BS; 5) otherwise, the user replies to the BSs requesting JT from the primary and the secondary BSs. Then, the BSs use a predetermined look up table to select the appropriate LED clusters for transmission. With a given BS cooperation set, the look up table provides the tuples of LED clusters that are used to serve the MS using JT. For example, if the cooperation set includes BSs A, B and C, the LED clusters which cover the region closest to the common vertex shared by cell A, B and C are selected to provide JT.

C. Frequency Planning

Since the magnitude response of the channel is flat, scheduling is simplified. We assume that the subcarriers are evenly distributed among the user population in the coverage area. Fig. 2 illustrates the frequency reuse pattern. For the first plan shown in Fig. 2 (A), the frequency band is divided into two subbands. The first subband is reused in each single point transmission region, while the second subband is reused in each multi-point JT region. The number of subcarriers in single point transmission subband N_{st} is set as follows:

$$N_{\text{st}} = \left\lceil \frac{A_{\text{st}} N_{\text{band}}}{A_{\text{total}}} \right\rceil, \tag{7}$$

where A_{st} denotes the total combined area of single point transmission regions, A_{total} denotes the total coverage area and N_{band} denotes the number of all subcarriers. The number of subcarriers in the JT subband, N_{jt}, is calculated by (8) as

$$N_{\text{jt}} = N_{\text{band}} - N_{\text{st}}. \tag{8}$$

This frequency allocation plan ensures spatially uniform availability of frequency resources. This is to support the assumptions of a uniform user distribution as well as equal target data rate of all users in the network. However, there is no interference mitigation between adjacent JT regions. Therefore, low SINRs are achieved at the boundaries of two adjacent JT regions. For the second plan shown in Fig. 2 (B), the subband for JT regions is divided into two partitions as follows:

$$N_{\text{jt1}} = N_{\text{jt2}} = \lfloor (N_{\text{band}} - N_{\text{st}})/2 \rfloor. \tag{9}$$

The two JT subbands are reused in a pattern such that adjacent JT regions always use different subbands in order to mitigate CCI. The subband for single point transmission remains the same. This frequency plan offers improved receiver SINR performance, but fewer number of subcarriers are available in the JT regions. For convenience, the JT systems with frequency plan 1 and 2 are defined as JT1 system and JT2 system, respectively.

In a full frequency reuse system, the whole frequency band is permitted to be used in each cell. Within a cell coverage area (hexagon indicated by blue dashed line boundaries in Fig. 3), subcarriers are not reused. In a JT2 system, the entire set of subcarriers are prevented

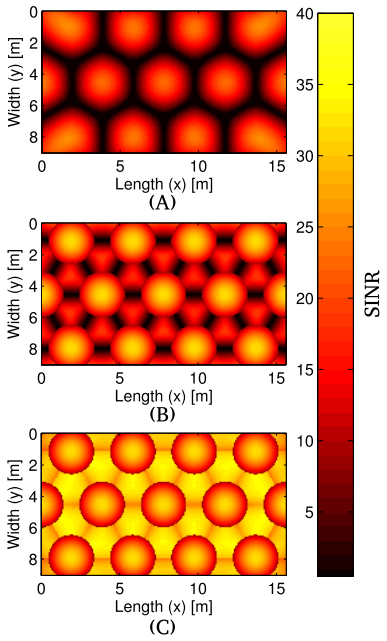

Fig. 5. SINR distribution of the system using (A) full frequency reuse (B) joint transmission 1 (C) joint transmission 2.

from being reused within the region bounded by red solid curves in Fig. 3. The area of this region is exactly equal to the coverage area of a cell. Therefore, the reuse factor of a JT2 system is equivalent to the one in a full frequency reuse system.

IV. Results and Discussions

A. Simulation setup

The investigated downlink cellular network scenario is deployed in a 15.6 m $\times$ 9 m $\times$ 3 m office room with a total of 13 LED arrays. It is assumed that mobile devices with a PD receiver are located 0.85 m above the floor, which is the typical height of a desk top. All PD receivers are facing upward towards the ceiling. The IFFT/FFT size of the applied OFDMA system is 512. For simplicity, no power control is applied and all LEDs have the same average optical transmit power. The phosphor-based white LED described in [9] is used in the system model. Since only the optical power of blue light is used for communication purposes, the effective optical power is 50% of the total power. 40 users are uniformly distributed in the room. Key simulation parameters are listed in Table I. Because the main contribution of this paper is to demonstrate the potential gain in terms of SINR and throughput achieved by JT systems, some of the system parameters including $\Phi_{1/2}$, α, γ_{th} and Ψ_c are determined empirically in order to guarantee reasonable system performance while it is recognised that an optimisation of these parameters would potentially further enhance the system performance.

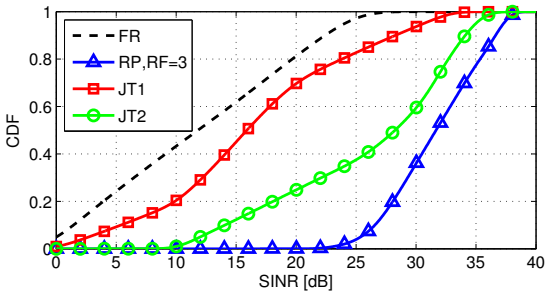

Fig. 6. Cumulative distribution function of received SINR. FR refers to full frequency reuse system, RP, RF=3 refers to static resource partitioning system with a reuse factor of three, JT1 refers to joint transmission system 1 and JT2 refers to joint transmission system 2.

B. Benchmark systems

The JT systems are compared against two benchmark systems. One of the benchmark systems uses full frequency reuse (FR) with a reuse factor of one. The other system uses traditional static resource partitioning (RP) with a reuse factor of three [2]. The simulation parameters for them are the same as for the JT systems in order to guarantee a fair comparison.

C. Illumination function

For a VLC system, it is important to fulfil the lighting requirements. Fig. 4 illustrates that the majority of the area (more than 90%) in the room benefits from illuminance within the required range. For better lighting performance, extra lighting fixtures without communication function can be installed to complement the low illuminance at room edges.

D. Receiver SINR

Fig. 5 shows the SINR distribution for the different systems. The benchmark FR system achieves the worst SINRs. For the JT1 system, the cell-edge SINRs are improved compared to the FR system, especially for the users near the centre of JT regions. However, due to the lack of interference mitigation between adjacent JT regions, the users at the boundaries between adjacent JT regions achieve poor SINR. In contrast, in the JT2 system, the same frequency band is not reused in adjacent JT regions. Therefore, the cell-edge user SINR is further improved (above 30 dB) compared to the JT1 system at the cost of spectrum reuse. Fig. 6 presents the cumulative distribution function (CDF) of the SINRs in different systems. It demonstrates that JT1 and JT2 systems exhibit a 4.1 dB and a 16.4 dB improvement, respectively, in terms of median SINR relative to an FR system.

E. Downlink throughput

Fig. 7 and Fig. 8 show the CDF of the downlink system throughput and the user throughput in the dif-

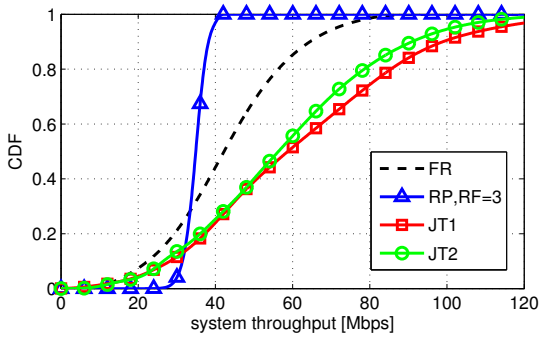

Fig. 7. Cumulative distribution function of the system throughput.

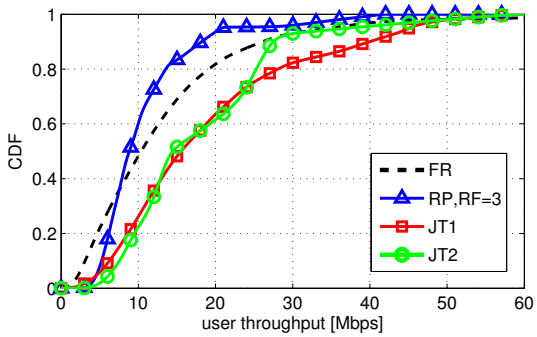

Fig. 8. Cumulative distribution function of the user throughput.

ferent systems. The system throughput is defined as the aggregate data rate in the given optical cell, while the user throughput is defined as the transmission data rate achieved by a single MS. With the largest reuse factor, the RP system achieves the lowest median system throughput of 34.9 Mbps. In contrast, an FR system with a reuse factor of one achieves a higher median system throughput of 42.3 Mbps. As discussed in section III-C, the JT2 system has the same reuse factor as the FR system. In addition, the JT2 system exhibits strong robustness to CCI. Therefore, the JT2 technique achieves a median system throughput of 56.3 Mbps, which is significantly higher than both the FR and the RP systems. However, the maximum number of subcarriers a user could use is determined by his location and is limited by the size of the respective subband. Therefore, the peak user throughput for the JT2 system is lower than the JT1 system. Since the JT1 system enforces a more aggressive frequency reuse, it achieves the highest median system throughput of 58.5 Mbps. The JT1 and the JT2 systems show a 67.6% and a 61.3% improvement compared to the RP system, respectively. The JT scheme also shows improvement in terms of the guaranteed user throughput (defined as the minimum data rate with 90% confidence) compared to the benchmarks. The JT1 and the JT2 systems achieve a 6.3 Mbps and a 7.5 Mbps guaranteed user throughput, respectively. These numbers are 100% to 140% higher than the guaranteed user throughput achieved by an FR system.

V. Conclusions

This paper addressed multi-point joint transmission in indoor optical atto-cell networks in order to achieve seamless coverage, high data rate and multiple access. The performance of a cellular system that applies joint transmission was compared to the performance of a full frequency reuse system and a static resource partitioning system with a reuse factor of three. The results showed that the joint transmission systems achieved higher cell-edge SINRs compared to a full frequency reuse system. In addition, a joint transmission system also achieved 67.6% improvement in terms of median system throughput compared to a static resource partitioning system. However, the downside of joint transmission systems is that they need extra signalling overhead.

Acknowledgement

Prof. Haas acknowledges support from the Engineering and Physical Sciences Research Council (EPSRC) under Established Career Fellowship grant EP/K008757/1.

References

[1] H. Elgala, R. Mesleh, and H. Haas, "Indoor Optical Wireless Communication: Potential and State-of-the-Art," *IEEE Commun. Mag.*, vol. 49, no. 9, pp. 56–62, Sep. 2011, ISSN: 0163-6804.

[2] G. W. Marsh and J. M. Kahn, "Channel Reuse Strategies for Indoor Infrared Wireless Communications," *IEEE Transactions on Communications*, vol. 45, no. 10, pp. 1280–1290, Oct. 1997.

[3] B. Ghimire and H. Haas, "Self Organising Interference Coordination in Optical Wireless Networks," *EURASIP Journal on Wireless Communications and Networking*, 2012, to appear.

[4] P. Baier, M. Meurer, T. Weber, and H. Tröger, H.ger, "Joint transmission (jt), an alternative rationale for the downlink of time division cdma using multi-element transmit antennas," in *IEEE Sixth International Symposium on Spread Spectrum Techniques and Applications*, vol. 1, 2000, pp. 1–5 vol.1.

[5] J. M. Kahn and J. R. Barry, "Wireless Infrared Communications," *Proceedings of the IEEE*, vol. 85, no. 2, pp. 265–298, Feb. 1997.

[6] G. Prince and T. Little, "On the performance gains of cooperative transmission concepts in intensity modulated direct detection visible light communication networks," in *2010 6th International Conference on Wireless and Mobile Communications (ICWMC)*, 2010, pp. 297–302.

[7] J. Armstrong, "OFDM for Optical Communications," *Journal of Lightwave Technology*, vol. 27, no. 3, pp. 189–204, Feb. 2009.

[8] S. Dimitrov and H. Haas, "Information rate of ofdm-based optical wireless communication systems with nonlinear distortion," *Journal of Lightwave Technology*, vol. 31, no. 6, pp. 918–929, 2013.

[9] J. Grubor, S. Randel, K.-D. Langer, and J. Walewski, "Bandwidth-efficient indoor optical wireless communications with white light-emitting diodes," in *6th International Symposium on Communication Systems, Networks and Digital Signal Processing*, 2008, pp. 165–169.

[10] S. Dimitrov, H. Haas, M. Cappitelli, and M. Olbert, "On the Throughput of an OFDM-based Cellular Optical Wireless System for an Aircraft Cabin," in *Proc. of European Conference on Antennas and Propagation (EuCAP 2011)*, Rome, Italy, 11–15 Apr. 2011, invited Paper.